Semi-analytical and analytical formulae for the classical loss in granular materials with rectangular and elliptical grain shapes

Olivier de La Barrière, M Lobue, F Mazaleyrat

Semi-analytical and analytical formulae for the classical loss in granular materials with rectangular and elliptical grain shapes

O. de la Barrière, M. LoBue, F. Mazaleyrat

SATIE, ENS Cachan, CNRS, UniverSud, 61 av du President Wilson, F-94230 Cachan, France

Granular soft magnetic materials, such as ferrites or Soft Magnetic Composites, are widely spread in modern electrical engineering applications. An important loss contribution is the classical one. It is known that in these materials, two kinds of classical loss must be distinguished: eddy currents flowing at the scale of the whole sample (therefore called macroscopic), and current lines inside the grains (called microscopic). For the macroscopic eddy currents computation, the sample cross sections are often square or rectangular. For eddy currents prediction inside the grains, two cases can be distinguished: the case of low density materials, for which circular or elliptical grain shapes are often realistic, and the case of high density materials. In this last class of granular materials, it is more difficult to identify a precise grain shape, because the deformations occurring during the compaction process often give to the grains a random shape. For carrying out the eddy current computation, rectangular shapes are often considered, because they allow a complete filling of the available space. To our knowledge, analytical eddy current formulae only exist for cylindrical or spherical regions. For other shapes such as squares, rectangles, or ellipses, the finite element method must be used to compute the eddy current distribution, which can be time consuming. This paper overcomes this difficulty by proposing respectively a semi-analytical formula for classical loss in rectangular geometries, and an analytical formula for elliptical cases.

***Index Terms*—classical loss computation, granular materials, rectangular shape, elliptical shape.**

I. Introduction

GRANULAR MAGNETIC MATERIALS, such as ferrites [*1*] or Soft Magnetic Composites (SMC) [*2*] are nowadays very popular in modern electrical engineering applications, such as electrical machines [*3*], or power electronics [*4*]. Indeed, these magnetic materials, made of magnetic particles coated by a dielectric insulator, potentially allow a significant reduction of the classical loss component [*5*][*6*], compared to laminated materials [*7*], in applications for which a magnetic permeability decrease is acceptable [*8*].

The starting point of the loss separation analysis [*9*] is an accurate computation of the classical loss component [*10*]. Actually, in granular materials, classical loss computation is far to be trivial. Indeed, it was shown that in these materials (ferrites or SMC), two classical loss terms must be distinguished [*5*][*2*][*11*]. The first one is linked to eddy currents flowing at the scale of the single particle (therefore called microscopic). The second term (called macroscopic) is due to eddy currents flowing at the scale of the whole sample, because of capacitive effects through the dielectric insulator, or random contacts appearing between grains during the compaction process. The two terms can be separately computed and summed up [*12*].

- For the microscopic loss component, analytical classical loss formulations are only available for cylindrical or spherical grains [*2*][*13*]. These shapes are realistic for low density materials [*2*]. However, it should be suitable, concerning low density materials, to also have formulae for elliptical grain shapes which can be encountered when dealing with anisotropic media [*11*]. For highly dense materials, such as SMC which undergo a high pressure compaction, it is more difficult to define a precise grain size. Indeed, the grains often take random shapes due to plastic deformations occurring during the compaction process [*14*]. For classical loss estimation, square or rectangular shapes seem quite realistic, because they allow a complete filling of the available space. Concerning ferrites, the rectangular shape is often taken for the grains when modeling the microscopic classical loss [*15*].
- Concerning the macroscopic classical loss prediction, the toroidal samples in which typical experiments are carried out often exhibit square or rectangular cross sections [*16*]. Therefore, the problem of eddy current computation in a square or rectangular region still arises (in this case, the resistivity to consider is the bulk resistivity of the sample, and the dimensions are the ones of the cross section).

This clearly emphasizes the need to accurately and efficiently compute the eddy current loss in a square, rectangular, or elliptical region. As no analytical classical loss formula exists for squares, rectangles, or ellipses, a finite element computation is often used to solve the Poisson equation [*14*]. This procedure can be quite cumbersome, and does not offer explicit expressions as analytical formulae.

The purpose of this paper is to propose respectively a semi-analytical formulation for the eddy current loss problem in a rectangular (or square) region, and an analytical solution in the elliptical one. This can be useful both for microscopic classical loss computation (in this case, the considered region is the grain, and the resistivity to consider is the one of the grain material), and for macroscopic eddy currents (then, the outer geometry of the region is the cross section, and the bulk resistivity of the material is used). In this paper, all computations are done under the hypothesis of skin depth much larger than the region edges. In the first part, the analytical method is detailed. In the second part, the results are

compared with finite elements, and approximation formulae are also worked out. Finally, as an example, these methods are applied to the microscopic eddy current computation for a SMC.

II. Analytical formulations

A. Problem to solve and simplifying assumptions

The simplifying assumptions are the followings.

- The eddy current paths are considered as bi-dimensional, flowing in the plane perpendicular to the flux density. The flux density is assumed purely alternative, i.e. applied in a given direction.
- The particle is assumed to be small enough to neglect skin effect in the range of frequencies of interest.

A Cartesian axis system *xyz* is introduced. The applied induction $B_a(t)$, which is also the local one since skin effect is ignored, is directed along the *z* axis, as well as the magnetic field $H(x,y,t)$, that can therefore be considered as a scalar. The current density $\vec{J}(x,y,t)=(J_x,J_y)$, on the contrary, is a vector located in the *xy* plane.

Under this set of simplifying assumptions, it has been shown in [*17*] that the equation giving the magnetic field is a Poisson equation:

$$\Delta H = \frac{\partial^2 H}{\partial x^2} + \frac{\partial^2 H}{\partial y^2} = \sigma \frac{dB_a}{dt} \tag{1}$$

where σ the conductivity of the material. The boundary condition on the region edges is $H=H_a(t)$, $H_a(t)$ being the external applied field. The problem to solve has been represented in Fig. 1. The rectangular has a width *L* along the *x* axis, and a height *l* along the *y* axis. For the elliptical shape, we take the major axis *A* along the *x* and the minor axis *B* along the *y* axis.

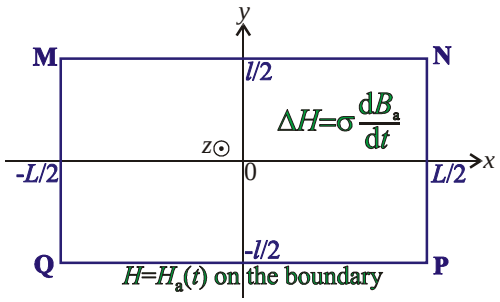

(a): Case of the rectangular region (width *L*, height *l*)

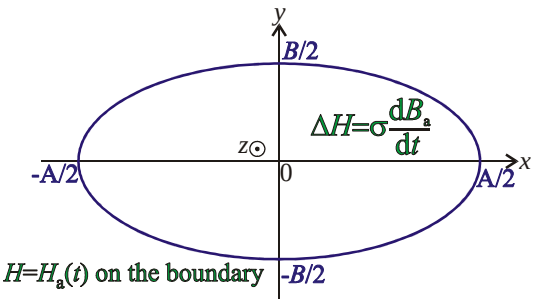

(b): Case of the elliptical region (major axis *A*, minor axis *B*)

Fig. 1: Bi-dimensional Poisson equation to solve, (a): rectangular region, and (b): elliptical region.

Once the magnetic field $H(x,y,t)$ is known, the current density can be obtained by the following partial derivations:

$$\begin{cases} J_x = \dfrac{\partial H}{\partial y} \\ J_y = -\dfrac{\partial H}{\partial x} \end{cases} \tag{2}$$

And the classical loss, in terms of energy lost per cycle of period *T* and per unit volume, is (*S* is the region cross section):

$$W_{\text{class}} = \int_0^T \frac{1}{S} \iint_{(S)} \frac{1}{\sigma} \left(J_x^2 + J_y^2 \right) dxdydt \tag{3}$$

B. Analytical developments

Expression (3) of the classical loss will be written, whatever the shape, under the following form (see the Appendix for a detailed explanation):

$$W_{\text{class}} = \sigma \cdot K \cdot S \cdot \int_{[T]} \left(\frac{dB_a}{dt} \right)^2 dt \tag{4}$$

In the previous expression, *K* is a factor depending on the region shape only (and not on its absolute dimensions). It can be shown that the expression (4) is valid for any region shape and size (provided skin effect can be neglected). In the following, we will give an analytical, or when not possible a semi-analytical (i.e. under the form of a converging infinite sum) expression of the shape factor *K*, for rectangular and elliptical grain shapes.

1) Rectangular and square shapes

In this case, a semi-analytical expression of the shape factor *K* is searched.

The solution of (1) is written:

$$H(x,y,t) = H_a(t) + H_1(x,t) + H_2(x,y,t) \tag{5}$$

The term $H_1(x,t)$ has been chosen to verify the Poisson equation, and only depends on the *x* coordinate. The following expression is proposed (this potential is chosen equal to zero on the segments MQ and NP of Fig. 1(a)):

$$H_1(x,t) = \frac{1}{2} \sigma \frac{dB_a}{dt} \left(x^2 - \frac{L^2}{4} \right) \tag{6}$$

The field $H_2(x,y,t)$ is harmonic (i.e. verifies $\Delta H_2=0$). It should be equal to zero on MQ and NP (Fig. 1(a)), and equal to the opposite of $H_1(x,t)$ on the segments MN and QP. $H_2(x,y,t)$ is made fictitiously periodic along the *x* direction, so the following mathematical expression can be proposed (the a_k functions are a family of unknown functions):

$$H_2(x,y,t)=\sum_{k=1}^{\infty}a_k(y,t)\cos\left((2k-1)\frac{\pi}{L}x\right) \quad (7)$$

Injecting (7) in the Laplace equation $\Delta H_2=0$, a second order differential equation is obtained for each a_k function:

$$\forall k\geq 1,\ \frac{\partial^2 a_k}{\partial y^2}-\left((2k-1)\frac{\pi}{L}x\right)^2 a_k(y,t)=0 \quad (8)$$

The solution of this equation is a linear combination of hyperbolic functions. The expression of $H_2(x,y,t)$ is therefore given by:

$$H_2(x,y,t)=\sum_{k=1}^{\infty}h_k(t)\left[\sinh\left((2k-1)\frac{\pi}{L}\left(y-\frac{L}{2}\right)\right)+\sinh\left((2k-1)\frac{\pi}{L}\left(y+\frac{L}{2}\right)\right)\right]\cdot\cos\left((2k-1)\frac{\pi}{L}x\right) \quad (9)$$

The set of functions $h_k(t)$ only depends on time. After an expansion of the field $H_1(x,t)$ into Fourier series of the x coordinate, the boundary condition $H_2(x,y=\pm l/2,t)=-H_1(x,t)$ on the segments MN and QP leads to the following expression, for the h_k coefficients:

$$h_k(t)=-\sigma\frac{dB_a}{dt}(-1)^{k-1}\frac{4L^2}{(2k-1)^3\pi^3\sinh\left((2k-1)\frac{\pi}{L}l\right)} \quad (10)$$

Knowing the terms $H_1(x,t)$ and $H_2(x,y,t)$ of (5), the currents J_x and J_y can be obtained by the derivation (2). The surface integral (3) can then be carried out to obtain the classical loss W_{class}. All computations made, and given the fact that the region cross section S is equal to $L.l$ for rectangular shapes, it turns out that the $K^{(RECT)}$ coefficient, which only depends on the height to width ratio $R=l/L$, is given by the following infinite series:

$$K^{(RECT)}=\frac{8}{\pi^4 R}\sum_{k=1}^{\infty}\left\{\frac{1}{(2k-1)^4}-\frac{2}{\pi R}\frac{1}{(2k-1)^5}\frac{\left[1-\exp\left(-(2k-1)\pi R\right)\right]^2}{\left[1-\exp\left(-2(2k-1)\pi R\right)\right]}\right\} \quad (11)$$

Equation (11) is an infinite sum. However, its numerical computation requires a finite number of terms. Therefore, the maximal number of terms is chosen using the following method: this number is increased until the partial sum do not change anymore, which means convergence of the computation (a relative difference of 0.5% is accepted). More precisely, calling $K_N^{(RECT)}$ the partial sum of the series (12) with N terms, $K_N^{(RECT)}$ is said to be equal to $K^{(RECT)}$ for the first number N verifying the condition:

$$\frac{\left|K_{N+1}^{(RECT)}-K_N^{(RECT)}\right|}{\left|K_N^{(RECT)}\right|}\leq 0.5\% \quad (12)$$

Using this criterion, as the series (11) exponentially converges, a maximal number of terms inferior to 20 is sufficient to compute $K^{(RECT)}$ whatever the R value. This can be achieved very rapidly, the computation time being divided by more than 100 in comparison with the finite element method to solve (1), which requires a cumbersome matrix inversion. This coefficient is plotted in Fig. 2 in function of $R=l/L$. This figures illustrates the fact that for a given excitation induction $B_a(t)$ and a given cross section S of the rectangle, the loss is reduced if the region exhibits a "flat" shape, that is to say if its height to width ratio is small. The maximal value is obtained for a square shape. Due to the fact that square shapes are often adopted in the literature [*11*], it might be interesting to give the numerical value of the coefficient for this particular case: $K^{(SQUARE)}=3.51\cdot10^{-2}$. An extended table of the $K^{(RECT)}$ coefficients in function of R is given in the Appendix.

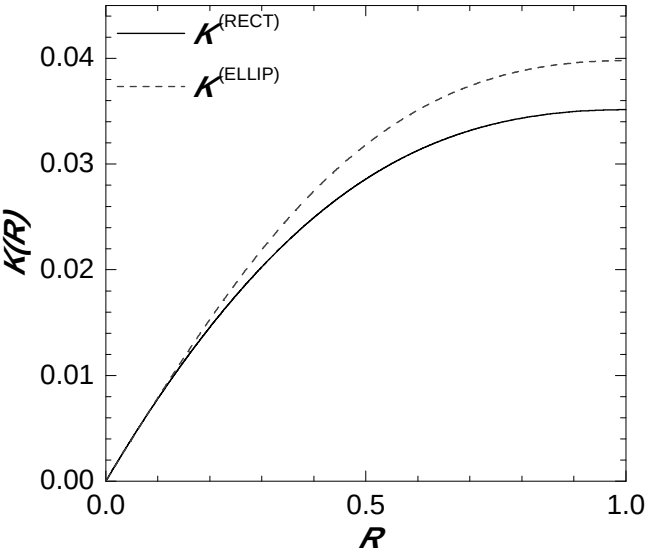

Fig. 2: Representation of the K coefficient in function of the ratio R (case of the rectangular for which $R=l/L$, and case of the ellipse for which $R=B/A$)

The validity of the previous approach can be also shown if the expression (11) asymptotically converges when $R\rightarrow 0$ towards the specific loss in a lamination. Indeed, a lamination is a rectangular whose width L is much larger than its height l. The smallest dimension l is kept constant, and the ratio $R=l/L$ tends towards zero. It is well known [*9*] that the specific loss in a lamination without skin effect is equal to:

$$W_{class}^{(LAM)}=\frac{\sigma\cdot l^2}{12}\int_{[T]}\left(\frac{dB_a}{dt}\right)^2 dt \quad (13)$$

Equation (4), in the case of a rectangular, can be written under the following form:

$$W_{\text{class}}^{(RECT)} = \sigma \cdot \frac{K^{(\text{RECT})}(R)}{R} \cdot l^2 \cdot \int_{[T]} \left(\frac{dB_a}{dt} \right)^2 dt \tag{14}$$

(13) and (14) are in correct agreement if the ratio $K^{(\text{RECT})}/R$ converges towards 1/12 when $R \to 0$. An asymptotic expansion to the third order gives:

$$\frac{\left[1-\exp\left(-(2k-1)\pi R\right)\right]^2}{\left[1-\exp\left(-2(2k-1)\pi R\right)\right]} \xrightarrow[R\to 0]{} \frac{(2k-1)\pi R}{2} - \frac{1}{24}\left[(2k-1)\pi R\right]^3 \tag{15}$$

Injecting (15) in (11) and dividing by R, it can be found:

$$\frac{K^{(RECT)}}{R} \xrightarrow[R\to 0]{} \frac{2}{3\pi^2} \sum_{k\geq 1} \frac{1}{(2k-1)^2} \tag{16}$$

A summation provides:

$$\sum_{k=1}^{\infty} \frac{1}{(2k-1)^2} = \frac{\pi^2}{8} \tag{17}$$

Finally, the following result can be established:

$$\frac{K^{(RECT)}}{R} \xrightarrow[R\to 0]{} \frac{1}{12} \tag{18}$$

(18) demonstrates the consistency between (11) and (13). This convergence can also be illustrated in Fig. 3.

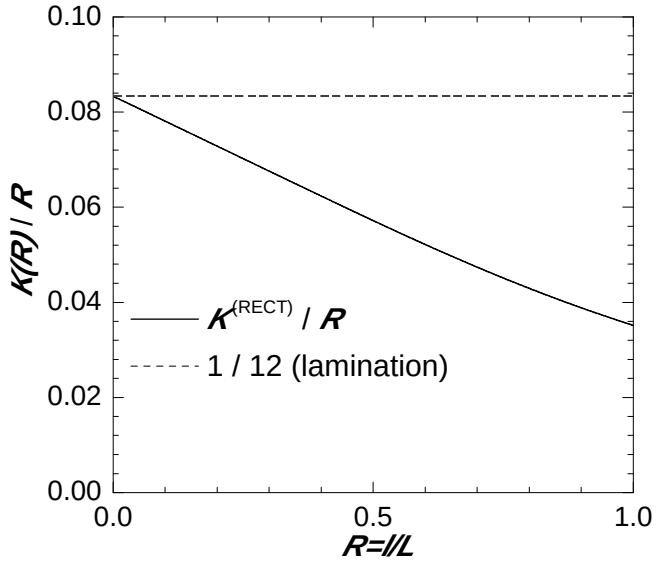

Fig. 3: Convergence of the ratio $K^{(\text{RECT})}/R$ towards 1/12 if $R \to 0$

2) Elliptical shapes

For non isotropic materials, the case of elliptical particles for the computation of microscopic classical loss can be of interest [*11*]. A is the major axis of the ellipse, and B is its minor axis. The ratio $R=B/A$ represents the shape factor of the elliptical particle, analogue to the ratio $R=l/L$ of the rectangular one. Calling $a = \sqrt{\left(A/2\right)^2 - \left(B/2\right)^2}$ and $r = \text{argtanh}(R)$, the analytical developments are carried out in the following $\rho\theta$ coordinate system:

$$\begin{cases} x = a \cdot \cosh(\rho) \cdot \cos(\theta) \\ y = a \cdot \sinh(\rho) \cdot \sin(\theta) \end{cases} \tag{19}$$

The Poisson equation becomes:

$$\frac{\partial^2 H}{\partial^2 \rho} + \frac{\partial^2 H}{\partial^2 \theta} = \sigma \frac{dB_a}{dt} \frac{a^2}{2} \left[\cosh(2\rho) - \cos(2\theta)\right] \tag{20}$$

Separating the variables ρ and θ, and taking into account the boundary conditions, the following solution can be found:

$$H(\rho,\theta) = H_a(t) + \frac{a^2}{8}\sigma \frac{dB_a}{dt}\left[\cosh(2\rho) - \cosh(2r) + \left(1 - \frac{\cosh(2\rho)}{\cosh(2r)}\right)\cos(2\theta)\right] \tag{21}$$

The derivation of this expression gives the current density components of (2) that can be substituted in (3). The integral of (3), performed on the elliptical cross-section, takes the form:

$$W_{\text{class}}^{(\text{ELLIP})} = \sigma \frac{a^2}{16}\left[\cosh(2r) - \frac{1}{\cosh(2r)}\right] \int_{[T]} \left(\frac{dB_a}{dt} \right)^2 dt \tag{22}$$

Therefore, the ellipse cross section being equal to $S=\pi/4 \cdot A \cdot B$, the $K^{(\text{ELLIP})}$ coefficient of formula (4), which is only dependant on the ratio $R=B/A$ and not on the absolute lengths A and B, has the following expression:

$$K^{(\text{ELLIP})} = \frac{1}{16\pi}\left[\frac{1}{\tanh(r)} - \tanh(r)\right]\left[\cosh(2r) - \frac{1}{\cosh(2r)}\right] \tag{23}$$

The previous expression has been represented in Fig. 2 in function of the shape factor $R=B/A$ for the ellipse (it is recalled that $r=\text{argtanh}(R)$). It is interesting to notice that for a given region cross section S, and for a given shape ratio R of the particle (equal to l/L for the rectangular and B/A for the ellipse), the loss is approximately 10% higher for the elliptical shape than for the rectangular shape.

It is recalled that for the circular case [*13*] (radius $A/2$), the loss is equal to:

$$W_{\text{class}}^{(\text{CIRCLE})} = \sigma \frac{1}{8} \left\langle \left(\frac{dB_a}{dt} \right)^2 \right\rangle_{[T]} \left(\frac{A}{2} \right)^2 \tag{24}$$

This means that the $K^{(\text{CIRCLE})}$ factor for the circle is equal to $1/(8\pi) \approx 3.98 \cdot 10^{-2}$. As shown in Fig. 2, this is the limit of expression (23) when $R=B/A \to 1$.

III. NUMERICAL RESULTS AND SIMPLIFIED FORMULATIONS

A. *Finite element verification*

The Poisson equation (1) can also be solved by finite elements (FEM)[1], and the obtained loss or K factor can be compared to the one provided by the analytical method. This verification is shown in Fig. 4 for what concerns the $K^{(RECT)}$ factor of the rectangular. Exact correspondence can be observed. However, the computation time is more than 100 times faster for the semi-analytical method.

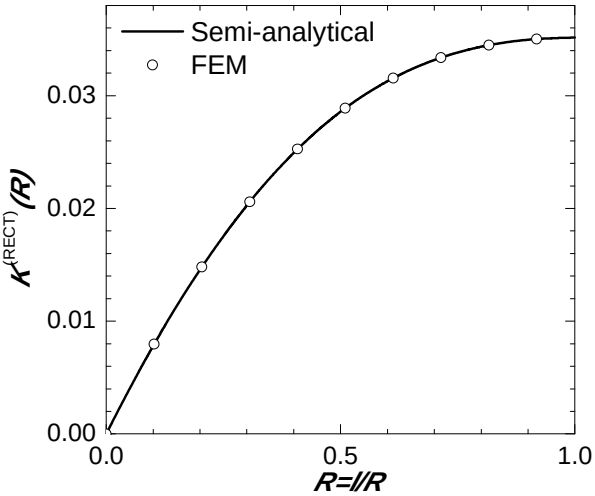

Fig. 4: Computation of the $K^{(RECT)}$ coefficient in function of the ratio $R=l/L$, by the semi-analytical formula (11), and by FEM

The current lines can also be computed by the analytical method, and the FEM method (they are the iso-level lines of the field H over the cross section). The results are shown in Fig. 5 for the rectangular case. The analytical and FEM results are also very similar.

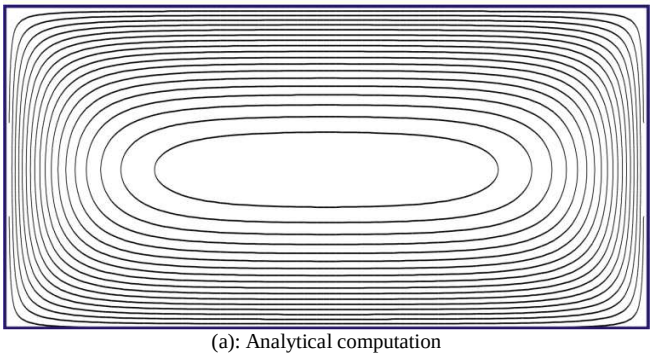

(a): Analytical computation

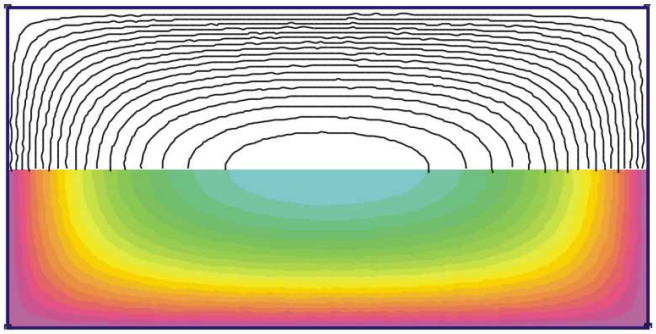

(b): FEM computation

Fig. 5: Current lines comparison between the analytical and FEM methods (rectangular of normalized absolute dimensions, normalized excitation dB_a/dt, and shape ratio $R=l/L$ equal to 1/2)

Similar results and conclusions can be found for elliptical regions.

B. *Simplified formulations for the rectangular*

Formula (11) provides an exact semi-analytical computation of the $K^{(RECT)}$ coefficient. However, the fact it is given under the form of an infinite series can be a limit for its practical use. In this section, we propose a very simple analytical formula for the loss in rectangular shapes, based on a simplification of (11). This simplified formula is compared with other existing simplified formulae for the loss in rectangular regions available in the literature.

The simplified formula we propose is based on the fact that the ratio $K^{(RECT)}/R$, represented in Fig. 3 as a function of R, looks like a linear curve with negative slope. A slope value equal to -1/20 has been empirically determined to fit the ratio $K^{(RECT)}/R$ with a satisfying precision on the whole interval [0;1] for R. Taking into account, as demonstrated before, that when R tends towards 0, the ratio $K^{(RECT)}/R$ tends towards 1/12 (the lamination case), the following formula is proposed:

$$\frac{K^{(RECT)}}{R} = \frac{1}{12} - \frac{1}{20} \cdot R \qquad (25)$$

Some authors [*18*] have tried to compute the eddy current distribution in rectangular regions using the approximation of rectangular eddy current paths. These rectangular paths have the same height to width ratio than the region and the same center (Fig. 6).

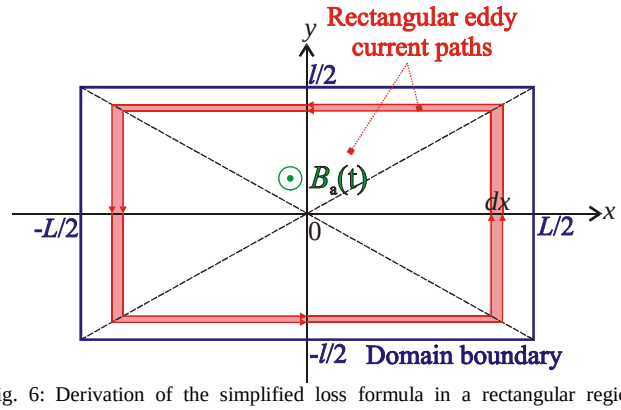

Fig. 6: Derivation of the simplified loss formula in a rectangular region presented in [*18*], based on the approximation of rectangular eddy current lines

[1] In this work, the free finite elements code FEMM, provided by the Foster-Miller company, has been used.

The conductance of an elementary current path as the one represented in Fig. 6 has the following expression (the vertical portions of this elementary current path are between the coordinates x and $x+dx$):

$$dG = \sigma \frac{R}{1+R^2} \frac{dx}{4x} \tag{26}$$

The RMS value of the electromotive force in the elementary current path is given by:

$$E(x) = 4Rx^2 \sqrt{\frac{1}{T}\int_{[T]} \left(\frac{dB_a}{dt}\right)^2 dt} \tag{27}$$

The classical loss in the region is therefore given by integration:

$$W_{\text{class}}^{(\text{BUNET})} = T\frac{1}{S}\int_0^{L/2} E^2 dG \tag{28}$$

After calculation, it is obtained:

$$W_{\text{class}}^{(\text{BUNET})} = \sigma \cdot \frac{1}{16} \cdot \frac{R}{1+R^2} \cdot S \cdot \int_{[T]} \left(\frac{dB_a}{dt}\right)^2 dt \tag{29}$$

This implies a $K^{(\text{BUNET})}$ factor equal to:

$$K^{(\text{BUNET})} = \frac{1}{16} \cdot \frac{R}{1+R^2} \tag{30}$$

Although simple, it is clear that the formula (30), contrary to (11), fails to reproduce the loss behaviour observed for a lamination, i.e. when $R \to 0$. Indeed, it has been shown in Section II.B.1) that the ratio K/R should tend towards 1/12 when $R \to 0$ to correctly reproduce the lamination behaviour, while from formula (30), $K^{(\text{BUNET})}/R \to 1/16$. This error comes from the fact that the assumption of concentric current lines with the same height to width ratio than the region is wrong for small ratios $R=l/L$.

The exact formula (11), the approximate one (25), and the one of Bunet (30) are compared in Fig. 7 (in terms of the K/R ratio). Although conceptually and analytically simple, the formula of Bunet (30) is quite far from the exact analytical result. The linear approximation (25) appears to be accurate on the whole range R, which is a clear advantage.

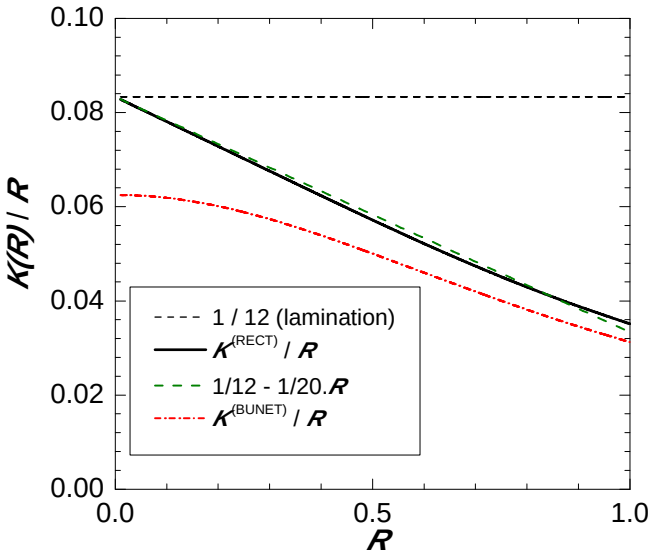

Fig. 7: K/R ratio in function of R obtained for the rectangular (limit case of the lamination when $R \to 0$, exact formula $K^{(\text{RECT})}/R$ (11), linear approximation (25), and $K^{(\text{BUNET})}/R$ ratio obtained by Bunet (30))

C. Application: computation of the microscopic classical loss in a Soft Magnetic Composite using a statistical model of the grain sizes and shapes

In [*19*], a method has been proposed to compute the classical loss in soft magnetic composites. It is based on a statistical analysis of micrographs such as the one shown in Fig. 8. As done in [*19*], the sample size is assumed to be small enough to neglect the macroscopic classical loss contribution (i.e. the currents flowing from grain to grain at the scale of the sample). Only microscopic eddy currents flowing at the scale of the grain are taken into account. Therefore, the region to consider in the computations is the single grain. As the grains are made of pure iron, the conductivity to consider is the one of iron $\sigma_{\text{Fe}}=9.93 \cdot 10^6$ S·m^{-1}.

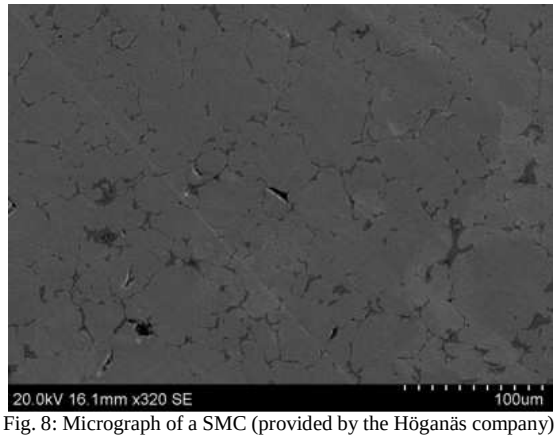

Fig. 8: Micrograph of a SMC (provided by the Höganäs company)

Using an image processing software, each grain has been isolated, and made equivalent to a rectangular of same cross section S, and same height to width ratio R (Fig. 9). The reason for choosing a rectangular shape is the important material density due to high pressure compaction, which cannot be obtained by an array of cylinders.

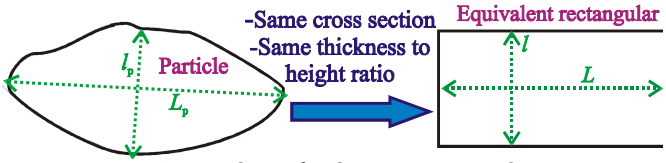

Fig. 9: Equivalence of each grain to a rectangular

Dealing with several micrographs and using appropriate statistical tools [*19*], a bivariate lognormal distribution (parameters (*S*,*R*)) has been identified for the material:

$$f(S,R)=\frac{1}{S\cdot R}\frac{1}{2\pi\xi_S\xi_R\sqrt{1-\chi_{S,R}}}\exp\left\{\frac{(\ln S-\alpha_S)^2}{\xi_S}+\frac{(\ln R-\alpha_R)^2}{\xi_R}-\frac{2\chi_{S,R}(\ln S-\alpha_S)(\ln R-\alpha_R)}{\xi_S\xi_R}\right\} \quad (31)$$

The classical loss is computed using the following integral:

$$W_{\text{class}}^{(SMC)}(J_p,f)=\sigma\cdot\int_{[T]}\left(\frac{dB_a}{dt}\right)^2 dt\cdot\int_0^\infty\int_0^\infty f(S,R)K^{(\text{RECT})}(R)S\cdot dRdS \quad (32)$$

The double integral in (*S*,*R*) has to be computed numerically. This can be time consuming if the $K^{(\text{RECT})}$ factor is computed using finite elements, because a quite important number of shape factor evaluations can be required for an accurate integral computation. This was the method followed in [*19*], and several minutes were required. On the contrary, using the simplified formula (25) for the *K* factor, the computation becomes instantaneous (less than one second), for a similar accuracy (Fig. 10). This case for which a statistical distribution of the grain sizes is used is a typical case for which a simplified analytical formula for the $K^{(\text{RECT})}$ coefficient (like (25)) is valuable from the computational point of view.

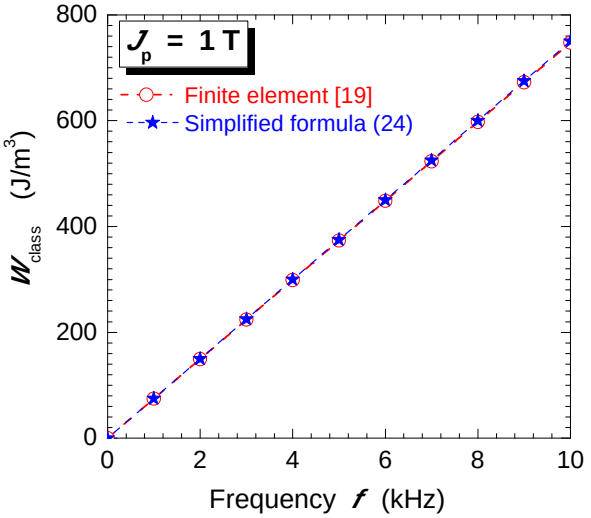

Fig. 10: Classical loss in the SMC of Fig. 8 in function of the frequency, for a peak polarization J_p=1 T (use of the finite element method to compute *K* [*19*], and use of the simplified formula (25))

IV. Conclusion

In this paper, a semi-analytical formula for the classical loss in rectangular-shaped regions and an analytical formula in elliptical ones have been proposed. It has been shown that the formula for the rectangular tends towards the well-known loss expression in laminations if the height to width ratio of the rectangular tends towards zero. Finite element validations are also proposed. The loss expression in rectangular regions can be both used for the computation of the macroscopic classical loss component (i.e. currents flowing at the scale of the sample which exhibits a rectangular cross section), and for microscopic classical loss evaluation for highly compacted materials. Elliptical shapes are useful for microscopic loss prediction in low density materials with anisotropy. An important decrease of the computation time compared to conventional methods such as finite elements has been observed.

In the second part of the article, a very simplified linear formula has been proposed for the classical loss in rectangular regions. This formula has been applied to rapidly and accurately compute the microscopic classical loss in a SMC, which requires a statistical computation to take into account the various shapes and sizes of the grains. The statistical properties of the grain have been retrieved by micrograph analysis.

V. Appendix

A. Explanation on formula (4)

Rather than using the magnetic field *H(x,y,t)* in this section, it is more convenient to use the electric vector potential *T(x,y,t)* chosen as:

$$T(x,y,t)=H(x,y,t)-H_a(t) \quad (33)$$

In this way, the Poisson equation (1) written in terms of electric vector potential *T* verifies homogeneous boundary conditions on the domain boundary Γ:

$$\begin{cases}\Delta T=\sigma\dfrac{dB_a}{dt}\\ T|_\Gamma=0\end{cases} \quad (34)$$

The current density is given by the same spatial derivatives as with the magnetic field:

$$\begin{cases}J_x=\dfrac{\partial T}{\partial y}\\ J_y=-\dfrac{\partial T}{\partial x}\end{cases} \quad (35)$$

Consider a region of arbitrary shape Ω (spatial coordinates *(x,y)*), and normalize it to a region Ω_n (normalized coordinates (x_n,y_n)), chosen in such a way that the domain cross-section S_n in the normalized coordinate system is equal to 1. The homothetic factor between the normalized region Ω_n and the real region Ω has the dimension of a length and is called *k* (Fig. 11). The cross-section of Ω is equal to $S=k^2$.

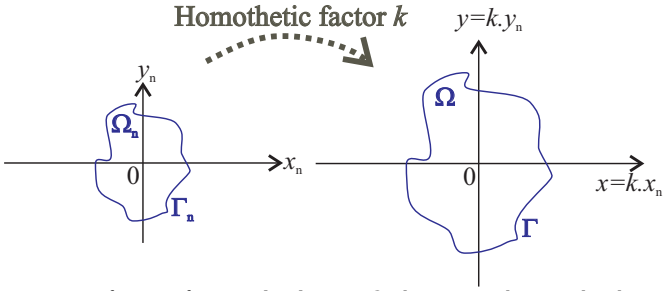

Fig. 11: Definition of a normalized region Ω_n chosen in such a way that the normalized cross-section S_n is equal to 1

In the real region Ω, the electric potential $T(x,y,t)$ is obtained solving (34) in the (xy) system. In the normalized coordinate system (x_n,y_n), one can find the normalized potential $t(x_n,y_n)$ verifying the following Poisson equation:

$$\begin{cases} \Delta_{(x_n,y_n)} t_n = \dfrac{\partial^2 t_n}{\partial x_n^2} + \dfrac{\partial^2 t_n}{\partial y_n^2} = 1 \\ t\big|_{\Gamma_n} = 0 \end{cases} \tag{36}$$

The following relation is clear:

$$\Delta_{(x,y)} = \frac{1}{k^2} \Delta_{(x_n,y_n)} \tag{37}$$

In addition, using the linearity of the Poisson equation, it can be obtained:

$$T(x,y,t) = k^2 \cdot \sigma \cdot \frac{dB_a}{dt} \cdot t(x_n, y_n) \tag{38}$$

Thus, the current density components are:

$$\begin{cases} J_x = k \cdot \sigma \cdot \dfrac{dB_a}{dt} \cdot \dfrac{\partial t}{\partial y_n}(x_n, y_n) \\ J_y = -k \cdot \sigma \cdot \dfrac{dB_a}{dt} \cdot \dfrac{\partial t}{\partial x_n}(x_n, y_n) \end{cases} \tag{39}$$

Carrying out the spatial and temporal means of (3), and remembering that $S=k^2$, it is found for the specific classical loss per cycle:

$$W_{\text{class}} = \sigma \cdot \left[\iint_{(S_n)} \left(\frac{\partial t}{\partial x_n} \right)^2 + \left(\frac{\partial t}{\partial y_n} \right)^2 dx_n dy_n \right] \cdot S \cdot \int_{[T]} \left(\frac{dB_a}{dt} \right)^2 dt \tag{40}$$

Therefore, noticing that the coefficient K defined as in (41) does not depend on the absolute dimensions of the region Ω, formula (4) is found.

$$K = \iint_{(S_n)} \left(\frac{\partial t}{\partial x_n} \right)^2 + \left(\frac{\partial t}{\partial y_n} \right)^2 dx_n dy_n \tag{41}$$

For example, for what concerns the lamination with very small height to width ratio $R=l/L$, the classical loss is given by (14). An obvious algebraic manipulation gives, since the cross section is equal to $S=L \cdot l$:

$$W_{\text{class}}^{(\text{LAM})} = \sigma \cdot \frac{1}{12} R \cdot S \cdot \int_{[T]} \left(\frac{dB_a}{dt} \right)^2 dt \tag{42}$$

The coefficient K in this important case of thin laminations is equal to $K=1/12 \cdot R$.

B. *Table of the $K^{(RECT)}$ coefficients in function of R*

An extended table of the $K^{(\text{RECT})}$ coefficients in function of R, computed from expression (11), is given in Table I:

TABLE I
$K^{(\text{RECT})}$ COEFFICIENTS IN FUNCTION OF R (EXPRESSION (11))

R	$K^{(\text{RECT})}$
0	0
0.1	$7.81 \cdot 10^{-3}$
0.2	$1.46 \cdot 10^{-2}$
0.3	$2.03 \cdot 10^{-2}$
0.4	$2.49 \cdot 10^{-2}$
0.5	$2.86 \cdot 10^{-2}$
0.6	$3.13 \cdot 10^{-2}$
0.7	$3.32 \cdot 10^{-2}$
0.8	$3.43 \cdot 10^{-2}$
0.9	$3.50 \cdot 10^{-2}$
1	$3.51 \cdot 10^{-2}$

VI. References

[1] A. Magni et al., "Domain wall processes, rotations, and high-frequency losses in thin laminations," *IEEE Transactions on Magnetics*, vol. 48, no. 11, pp. 3796-3799, 2012.

[2] M. Anhalt and B Weidenfeller, "Dynamic losses in FeSi filled polymer bonded soft magnetic composites," Journal of Magnetism and Magnetic Materials, vol. 304, no. 2, pp. e549-e551, 2006.

[3] Y. Guo, J. Zhu, H. Lu, Z. Lin, and Y. Li, "Core Loss Calculation for Soft Magnetic Composite Electrical Machines," IEEE Transactions on Magnetics, vol. 48, no. 11, pp. 3112-3115, 2012.

[4] R.A. Salas and J. Pleite, "Equivalent Electrical Model of a Ferrite Core Inductor Excited by a Square Waveform Including Saturation and Power Losses for Circuit Simulation," IEEE Transactions on Magnetics, vol. 49, no. 7, pp. 4257-4260, 2013.

[5] C. Appino et al., "Computation of eddy current losses in Soft Magnetic Composites," vol. 48, no. 11, pp. 3470-3473, 2012.

[6] A. Bordianu, O de la Barrière, O. Bottauscio, M. Chiampi, and A. Manzin, "A Multiscale Approach to Predict Classical Losses in Soft Magnetic Composites," IEEE Transactions on Magnetics, vol. 48, no. 4, pp. 1537-1540, 2012.

[7] F. Jiancheng, W. Xi, W. Tong, T. Enqiong, and F. Yahong, "Homopolar 2-Pole Radial Permanent-Magnet Biased Magnetic Bearing With Low Rotating Loss," IEEE Transactions on Magnetics, vol. 48, no. 8, pp. 2293-2303, 2012.

[8] C. Cyr, P. Viarouge, S. Clenet, and J. Cros, "Methodology to study the influence of the microscopic structure of soft magnetic composites on their global magnetization curve," IEEE Trasactions on magnetism, vol. 45, no. 3, pp. 1178-1181, 2009.

[9] G. Bertotti, "General properties of power losses in soft ferromagnetic materials," IEEE Transactions on Magnetics, vol. 24, no. 1, pp. 621-630, 1988.

[10] A. Magni et al., "Magnetization Process in Thin Laminations up to 1 GHz," IEEE Transactions on Magnetics, vol. 48, no. 4, pp. 1363-1366, 2012.

[11] O. Bottauscio, A. Manzin, V. Chiadó Piat, M. Codegone, and M. Chiampi, "Electromagnetic phenomena in heterogeneous media: Effective properties and local behavior," Journal of Applied Physics, vol. 100, no. 4, pp. 044902-1--044902-8, 2006.

[12] C. Appino et al., "Classical eddy current losses in soft magnetic composites," Journal of Applied Physics, vol. 113, no. 7, p. 17A322, 2013.

[13] R.M. Bozorth, Ferromagnetism, Wiley, Ed., 1993.

[14] O. de la Barrière et al., "Loss separation in soft magnetic composites," Journal of Applied Physics, vol. 109, no. 7, p. 07A317, 2011.

[15] C. Beatrice, O. Bottauscio, M. Chiampi, F. Fiorillo, and A. Manzin, "Magnetic loss analysis in Mn–Zn ferrite cores," Journal of Magnetism and Magnetic Materials, vol. 304, no. 2, pp. e743-e745, 2006.

[16] M. LoBue, V. Loyau, and F. Mazaleyrat, "Analysis of volume distribution of power loss in ferrite cores," Journal of Applied Physics, vol. 109, no. 7, pp. 07D308-1-07D308-3, 2011.

[17] G. Bertotti, Hysteresis in Magnetism, Academic Press, Ed., 1998.

[18] P. Bunet, Courants de Foucault. Paris: Librairie J.B. Baillière et fils, 1933.

[19] O. de la Barrière et al., "Characterization and prediction of magnetic losses in Soft Magnetic Composites under distorted induction waveform," IEEE Transactions on Magnetics, vol. 49, no. 4, pp. 1318-1326, 2013.